Complexes with short Sn–Co bonds; preparation, structures and bonding in Et₄N[*trans*-(Cl₃Sn)₂Co(CO)₃] and [Co{(pz)₃BH}₂][*trans*-{[(CO)₄Co]Cl₂Sn}₂Co(CO)₃]

Owen J. Curnow, Brian K. Nicholson * and Milton J. Severinsen

School of Science, University of Waikato, Private Bag, Hamilton (New Zealand)
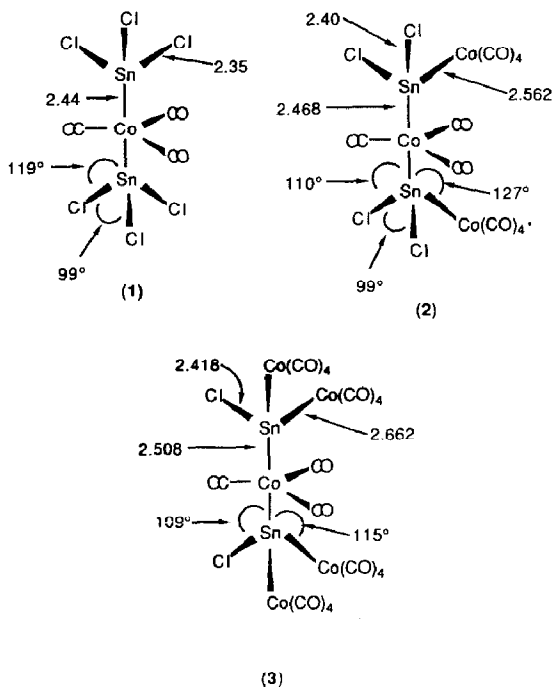
(Received December 11th, 1989)

Abstract

The reaction of [HB(pz)₃]SnCl₃ (pz = 1-pyrazolyl) with [Co(CO)₄]⁻ gave a mixture of products from which the anion [*trans*-{[(CO)₄Co]Cl₂Sn}₂Co(CO)₃]⁻ (**2**) was isolated as the [Co{(pz)₃BH}₂]⁺ salt, and characterised by X-ray crystallography. Reactions of [H₂B(pz)₂]SnCl₃ with [Co(CO)₄]⁻, and of ClSn[Co(CO)₄]₃ with K[HB(pz)₃] or K[H₂B(pz)₂], were also investigated. For comparison with **2**, the anion [*trans*-(Cl₃Sn)₂Co(CO)₃]⁻ (**1**) was made from Cl₃SnCo(CO)₄ and [SnCl₃]⁻ and structurally characterised as its Et₄N⁺ salt. In both **1** and **2** the Sn–Co bonds to the central cobalt atom are remarkably short (2.444(1) and 2.468(1)Å, respectively).

Introduction

There are no examples of clusters involving a *closo*-SnCo₃ unit, although corresponding CCo₃, SiCo₃ and GeCo₃ units are well established [1–3]. This has been attributed to the relative sizes of the main group atoms, with tin being too large to adopt a μ_3-bridging position [1]. However *closo*-(μ_3-Bi)Co₃(CO)₉, with the large μ_3-Bi atom has been reported [4], and the trigonal bipyramidal cluster [μ_3-Sn{Fe(CO)₂Cp}]₂Fe₃(CO)₉ also contains *closo*-SnFe₃ units [5], so a SnCo₃ unit probably only awaits development of an appropriate method of synthesis.

In the expectation that six-coordinate tin might be incorporated more readily than a four-coordinate one into a *closo* cluster, we previously reacted the open ClSn[Co(CO)₄]₃ with the tridentate, all-*cis* chelating ligand [HB(pz)₃]⁻, (pz = 1-pyrazolyl). Instead of the expected cluster, the [Sn₂Co₅Cl₂(CO)₁₉]⁻ anion **3**, as its Co[(pz)₃BH]₂⁺ salt, formed in a complicated reaction sequence [6].

In this paper we describe a more detailed examination of these reactions. This has led to the structural characterisation of another anion, related to that previously described, namely [{[(CO)₄Co]Cl₂Sn}₂Co(CO)₃]⁻ (**2**) isolated as its [Co{(pz)₃

Cl
Cl—Sn—Cl —2.35
2.44 →
OC—Co—CO
       CO
119° → Sn
Cl   Cl
    Cl
99°
(1)

2.40
Cl
Cl—Sn—Co(CO)₄
       —2.562
2.468 →
OC—Co—CO
       CO
110° → Sn —127°
Cl   Co(CO)₄·
    Cl
99°
(2)

2.418
Cl—Sn—Co(CO)₄
       Co(CO)₄
       —2.662
2.508 →
OC—Co—CO
       CO
109° → Sn —115°
Cl   Co(CO)₄
    Co(CO)₄
(3)

BH}₂]⁺ salt. To provide a more extended series for discussion we have made, and structurally characterized, the [(Cl₃Sn)₂Co(CO)₃]⁻ (1) ion.

Experimental

All reactions were performed under nitrogen in standard Schlenk equipment. Infrared spectra were recorded on a Perkin Elmer 180 spectrometer.

K[H₂B(pz₂] and K[HB(pz)₃] [7], [H₂B(pz)₂]SnCl₃ and [HB(pz)₃]SnCl₃ [8], Cl₃SnCo(CO)₄ [9], Cl₂Sn[Co(CO)₄]₂ [10], ClSn[Co(CO)₄]₃ [11] and Sn[Co(CO)₄]₄ [9] were prepared by published methods. [Et₄N][SnCl₃] (m.p. 79–81°C) was prepared by mixing stoichiometric amounts of anhydrous SnCl₂ and Et₄NCl · H₂O in ethanol.

Reaction of [HB(pz)₃]SnCl₃ with [Co(CO)₄]⁻. A solution of Na[Co(CO)₄] in thf (0.48 mmol in 2.7 ml) was added to a suspension of [HB(pz)₃]SnCl₃ (0.18 g, 0.41 mmol) in thf, producing a deep red solution. After 30 min the solvent was evaporated to leave a red/purple residue (ν(CO) (CH₂Cl₂) 2083m, 2069m, 2060w, 2002s, 1958w), which was extracted with CH₂Cl₂. Benzene was added to the extract, which was then cooled to produce orange-brown needles of [Co({(pz)₃BH}₂] [Sn₂Co₃Cl₄(CO)₁₁], containing 2, identified by X-ray crystallography (0.08 g, 10%) m.p. > 250°C, ν(CO) (CH₂Cl₂) 2094m sh, 2087s, 2069w, 2052m, 2034w, 2010vs, 1967m cm⁻¹. None of the other components in the mixture could be isolated.

Reaction of Cl₂Sn[Co(CO)₄]₂ with K[HB(pz)₃]. A solution of K[HB(pz)₃] (0.150 g, 0.595 mmol) in CH₂Cl₂ was added to a stirred solution of Cl₂Sn[Co(CO)₄]₂ (0.63 g, 1.19 mmol) in CH₂Cl₂. After 20 h all of the starting complex had been consumed. After evaporation, a hexane extraction of the residue removed ClSn[Co(CO)₄]₃,

identified by IR spectroscopy [11]. The remaining solid was dissolved in CH_2Cl_2, and the infrared spectrum showed only the carbonyl stretching bands of the $[Sn_2Co_3Cl_4(CO)_{11}]^-$ anion **2**.

Reaction of $ClSn[Co(CO)_4]_3$ with $K[H_2B(pz)_2]$. A solution of $ClSn[Co(CO)_4]_3$ (0.508 g, 0.75 mmol) in CH_2Cl_2 was treated with $K[H_2B(pz)_2]$ (0.19 g, 1.02 mmol) in CH_2Cl_2. After 1.5 h the solvent was removed from the blood-red solution. A hexane extract of the residue contained only red $Sn[Co(CO)_4]_4$ (by IR [9]). The remaining solid was dissolved in CH_2Cl_2 to give an intense blue-green solution with $\nu(CO)$ bands at 2078s, 2069m, 2064s, 2014s, 2001s, 1943w, 1937w, indicating the presence of $Sn[Co(CO)_4]_4$ and $[Sn_2Co_5Cl_2(CO)_{19}]^-$ (**3**), (though neither of these are blue-green!), but no other species could be definitely identified.

Reaction of $Sn[Co(CO)_4]_4$ with $K[HB(pz)_3]$. A CH_2Cl_2 solution of $K[HB(pz)_3]$ (0.16 g, 0.62 mmol) was added to a stirred solution of $Sn[Co(CO)_4]_4$ (0.25 g, 0.10 mmol) in the same solvent. This gave a very air-sensitive deep green solution with $\nu(CO)$ bands at 2082m, 2065s, 2056w, 1994vs, 1970w cm^{-1}. No characterisable metal carbonyl species could be isolated, although some $Co[(pz)_3BH]_2$ was identified [12].

The corresponding reaction between $Sn[Co(CO)_4]_4$ and $K[H_2B(pz)_2]$ in thf gave a green solution with the same infrared spectrum.

Reaction of $[H_2B(pz)_2]SnCl_3$ with $[Co(CO)_4]^-$. A solution of $Na[Co(CO)_4]$ (1.4 mmol) in thf (8 ml) was added to a suspension of $[H_2B(pz)_2]SnCl_3$ (0.15 g, 0.40 mmol). The solution immediately became bright red and then turned purple during 5 min. The solvent was evaporated and the solid dissolved in CH_2Cl_2 to give a deep green solution. Hexane was added and the solution cooled to give red crystals of $Sn[Co(CO)_4]_4$ and purple crystals of $Co[(pz)_2BH_2]_2$, which were identified spectroscopically [13] after manual separation. A dark green, very air-sensitive solid was also deposited ($\nu(CO)$ (CH_2Cl_2) 2079m, 2065s, 2055w, 1997vs,br, 1977w,sh, 1860w? cm^{-1}) but could not be characterised.

Preparation of $Et_4N[(Cl_3Sn)_2Co(CO)_3]$. An ethanol solution of $Et_4N[SnCl_3]$ (0.125 g, 0.35 mmol) was added to a stirred ethanol solution of $Cl_3SnCo(CO)_4$ (0.185 g, 0.47 mmol). After 10 min the solution was orange-brown. The solvent was evaporated and the residue dissolved in CH_2Cl_2 ($\nu(CO)$ 2097s, 2087m, 2040s, 2013vs,br, 1982s cm^{-1}). Slow diffusion of hexane into this solution gave orange-brown needles (0.05 g, 20%), $\nu(CO)$ 1991 vs,br, which were shown by X-ray crystallography to be of $Et_4N[(Cl_3Sn)_2Co(CO)_3]$ (see below).

X-ray crystal structure of $[Co\{(pz)_3BH\}_2][trans-\{[CO)_4Co]Cl_2Sn\}_2Co(CO)_3]$

Orange-brown crystals were obtained from CH_2Cl_2/benzene. Precession photography indicated Cc or $C2/c$ as possible space groups, and the latter was shown to be the correct one by the full analysis. Cell parameters and intensity data were obtained with a crystal of dimensions $0.33 \times 0.25 \times 0.03$ mm, on an Enraf Nonius CAD4 diffractometer with Zr filtered Mo-K_α X-rays (λ 0.7107 Å).

Crystal data. $C_{29}H_{20}B_2Cl_4Co_4N_{12}O_{11}Sn_2 \cdot C_6H_6$, $M = 1427.2$, monoclinic, space group $C2/c$, a 24.091(7), b 7.525(4), c 32.544(8) Å, β 118.52(9)°, U 5183.9 Å^3, D_0 1.80, D_c 1.83 g cm^{-3}, for $Z = 4$, F(000) 2776, μ(Mo-K_α) 23 cm^{-1}. T 291 K, transmission factors 0.999(max), 0.739(min).

A total of 3955 unique reflections in the range $2° < 2\theta < 46°$ were collected by ω scans. Of these 2817 had $I > 2\sigma(I)$ and were used in all calculations.

Table 1

Final positional parameters for [Co{(pz)$_3$BH}$_2$][Sn$_2$Co$_3$Cl$_4$(CO)$_{11}$]

Atom	x	y	z	Atom	x	y	z
Sn(1)	0.08219(2)	0.10741(6)	0.22532(1)	C(11)	0.0	0.352(2)	0.25
Co(1)	0.0	0.1175(2)	0.25	C(12)	0.0535(3)	0.15(1)	0.3031(3)
Co(2)	0.13071(4)	0.8311(1)	0.20901(3)	C(21)	0.0517(3)	0.787(1)	0.1636(3)
Co(3)	0.25	0.25	0.0	C(22)	0.1512(3)	0.7718(9)	0.2678(3)
Cl(1)	0.1713(1)	0.2801(2)	0.2782(1)	C(23)	0.1671(3)	0.6408(9)	0.1979(2)
Cl(2)	0.0513(1)	0.2810(3)	0.1559(1)	C(24)	0.1765(3)	0.909(1)	0.1980(2)
O(11)	0.0	0.504(1)	0.25	C(31)	0.2349(3)	0.5552(9)	0.0531(2)
O(12)	0.0891(3)	0.955(1)	0.3373(2)	C(32)	0.2230(3)	0.579(1)	0.0910(2)
O(21)	0.0036(3)	0.7566(9)	0.1342(2)	C(33)	0.2162(3)	0.4106(9)	0.1041(2)
O(22)	0.1650(3)	0.7273(8)	0.3050(2)	C(41)	0.1312(2)	0.0330(9)	0.9507(2)
O(23)	0.3088()2)	0.0244(7)	0.3090(2)	C(42)	0.0942(3)	0.929(1)	0.9622(2)
O(24)	0.2060(3)	0.0907(8)	0.1898(2)	C(43)	0.1230(3)	0.9311(9)	0.0102(2)
N(31)	0.2357(2)	0.3821(6)	0.0447(2)	C(51)	0.3633(3)	0.0326(9)	0.0620(2)
N(32)	0.2242(2)	0.2934(7)	0.0763(2)	C(52)	0.3853(3)	0.9341(9)	0.1032(2)
N(41)	0.3194(2)	0.4041(7)	0.0105(2)	C(53)	0.3375(3)	0.9397(9)	0.1140(2)
N(42)	0.1752(2)	0.0335(7)	0.0265(2)	B(1)	0.2249(3)	0.090(1)	0.0759(2)
N(51)	0.3059(2)	0.0922(6)	0.0494(2)	C(1)	0.5385(6)	0.135(2)	0.5286(4)
N(52)	0.2892(2)	0.0348(7)	0.0814(2)	C(2)	0.5100(6)	0.153(2)	0.4798(4)
				C(3)	0.4723(6)	0.014(2)	0.4521(4)

The structure was solved by direct methods (MULTAN [14]), and routinely developed, with the benzene solvate molecule being revealed in the penultimate difference map. In the final cycles of full-matrix least-squares refinement (SHELX-76 [15]) all of the atoms of the anion and the Co of the cation were treated anisotropically, while other atoms were assigned isotropic temperature factors. The hydrogen atoms of the cation were included in calculated positions (D(C–H, B–H) 0.98 Å) with a common temperature factor. Refinement converged at $R = 0.0319$, $R_w = 0.0346$, where $w = [\sigma^2(F) + 0.0008F^2]^{-1}$, with no final shifts greater than 0.35σ and no residual electron density > 0.55e Å^{-3}.

Table 2

Final positional parameters for Et$_4$N[(Cl$_3$Sn)$_2$Co(CO)$_3$]

Atom	x	y	z	Atom	x	y	z
Sn(1)	0.84235(2)	0.30779(3)	0.42689(2)	C(22)	0.75	0.9572(8)	0.0
Sn(2)	0.64535(3)	0.76939(3)	0.06596(2)	O(11)	0.9615(3)	0.1623(4)	0.6137(2)
Co(1)	0.75	0.3064(1)	0.50	O(12)	0.75	0.6088(5)	0.50
Co(2)	0.75	0.7719(1)	0.00	O(21)	0.9536(4)	0.6277(5)	0.1192(2)
Cl(11)	0.7234(1)	0.2315(1)	0.3072(1)	O(22)	0.75	1.0756(5)	0.00
Cl(12)	0.9021(1)	0.5213(1)	0.4021(1)	N	1.0075(3)	0.2195(3)	0.2537(2)
Cl(13)	1.0113(1)	0.1709(1)	0.4606(1)	C(31)	0.9602(4)	0.2615(5)	0.1764(2)
Cl(21)	0.6107(1)	0.9820(1)	0.1065(1)	C(32)	0.8292(4)	0.3000(5)	0.1336(3)
Cl(22)	0.7402(1)	0.6482(1)	0.1762(1)	C(41)	0.9394(4)	0.0956(4)	0.2577(2)
Cl(23)	0.4544(1)	0.6739(1)	0.0136(1)	C(42)	0.9420(4)	0.9676(5)	0.2186(3)
C(11)	0.8797(5)	0.2164(5)	0.5692(3)	C(51)	1.1399(4)	0.1840(5)	0.2856(2)
C(12)	0.75	0.4919(7)	0.50	C(52)	1.2059(4)	0.1383(5)	0.3631(2)
C(21)	0.8740(5)	0.6821(5)	0.0725(3)	C(61)	0.9921(4)	0.3357(5)	0.2947(3)
C(62)	1.0494(4)	0.4719(5)	0.2940(3)				

Table 3

Selected structural parameters for anions **1** and **2**

	$[(Cl_3Sn)_2Co(CO)_3]^-$ **(1)**		$[\{(CO)_4Co]Cl_2Sn\}_2Co(CO)_3]^-$ **(2)**			
	Anion 1	Anion 2				
Sn(1)–Co(1)	2.444(1)	2.441(1)	Sn(1)–Co(1)	2.468(1)	Sn(1)–Co(2)	2.562(1)
Sn(1)–Cl(1)	2.352(1)	2.366(1)	Sn(1)–Cl(1)	2.394(2)	Sn(1)–Cl(2)	2.401(2)
Sn(1)–Cl(2)	2.360(1)	2.359(1)				
Sn(1)–Cl(3)	2.338(1)	2.327(1)				
Sn(1)–Co(1)–Sn(1')	179.4(1)	178.9(1)	Sn(1)–Co(1)–Sn(1')	176.5(1)	Co(1)–Sn(1)–Co(2)	127.5(1)
Co(1)–Sn(1)–Cl(1)	117.0(1)	119.0(1)	Co(1)–Sn(1)–Cl(1)	109.5(1)	Co(1)–Sn(1)–Cl(2)	110.7(1)
Co(1)–Sn(1)–Cl(2)	119.1(1)	116.3(1)	Co(2)–Sn(1)–Cl(1)	104.4(1)	Co(2)–Sn(1)–Cl(2)	102.3(1)
Co(1)–Sn(1)–Cl(3)	119.8(1)	120.0(1)	Cl(1)–Sn(1)–Cl(2)	98.6(1)		
Cl(1)–Sn(1)–Cl(2)	97.3(1)	98.7(1)				
Cl(1)–Sn(1)–Cl(3)	98.3(1)	99.3(1)				
Cl(2)–Sn(1)–Cl(3)	101.2(1)	99.5(1)				
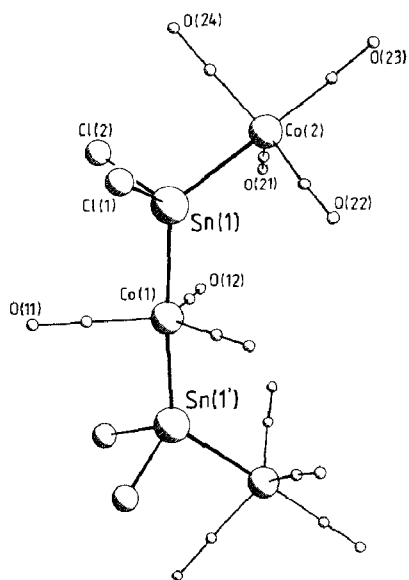
Fig. 1. (left) A general view of the anion $[\{[(CO)_4Co]Cl_2Sn\}_2Co(CO)_3]^-$ (2) showing atom labelling. There is a crystallographic 2-fold axis coincident with the Co(1)C(11)O(11) vector.
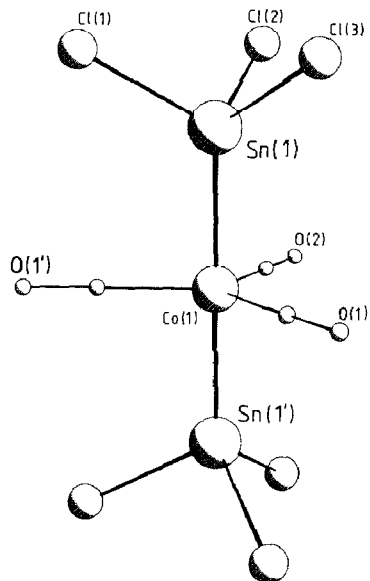
Fig. 2. (right) The structure of one of the independent anions $[(Cl_3Sn)_2Co(CO)_3]^-$ (1). There is a crystallographic 2-fold axis coincident with the Co(1)C(2)O(2) vector.
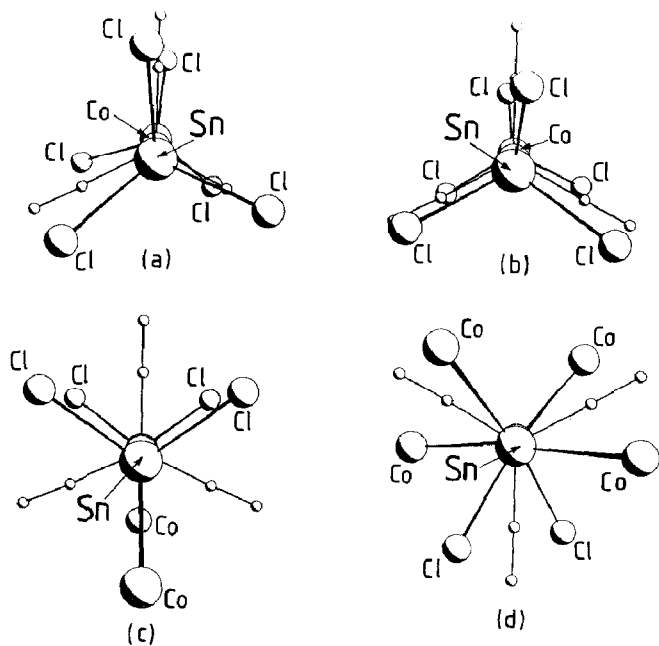

Fig. 3. The relative conformations of the anions: (a) and (b) $[(Cl_3Sn)_2Co(CO)_3]^-$ (1) (both independent forms); (c) $[\{[(CO)_4Co]Cl_2Sn\}_2Co(CO)_3]^-$ (2); and (d), $[\{[(CO)_4Co]_2ClSn\}_2Co(CO)_3]^-$ (3), (taken from ref. 6).

The final positional parameters are given in Table 1, selected bond parameters for the anion are given in Table 3, and the anion geometry is illustrated in Figs. 1 and 3.

X-ray crystal structure of $Et_4N[(Cl_3Sn)_2Co(CO)_3]$

Orange-brown crystals were obtained from CH_2Cl_2/hexane. Precession photography indicated a monoclinic primitive lattice. Cell parameters and intensity data were obtained with a crystal of dimensions $0.58 \times 0.39 \times 0.13$ mm, on an Nicolet P3 diffractometer with monochromated Mo-K_α X-rays (λ 0.7107 Å).

Crystal data. $C_{11}H_{20}Cl_6CoNO_3Sn_2$, $M = 723.3$, monoclinic, space group $P2/a$ (non-standard setting of $P2/c$), a 13.054(2), b 9.639(3), c 21.750(3) Å, β 121.27(2)°, U 2339.2 Å^3, D_0 2.08, D_c 2.05 g cm^{-3}, for $Z = 4$, $F(000)$ 1384, μ(Mo-K_α) 33 cm^{-1}, T 150 K, transmission factors 0.670(max), 0.238(min).

A total of 3925 unique reflections in the range $4° < 2\theta < 52°$ were collected by ω scans. Of these 3616 had $I > 2\sigma(I)$ and were used in all calculations.

The structure was solved by automatic interpretation of the Patterson map (SHELXTL) to locate the metal atoms, and all other non-hydrogen atoms were revealed in a subsequent difference map. There are two independent anions in the unit cell, each lying on a two-fold crystallographic axis. In the final cycles of full-matrix least-squares refinement (SHELX-76 [15]) all atoms were treated aniso-tropically, with the hydrogen atoms included in calculated positions (D(C–H) 1.08 Å) with common isotropic temperature factors for each type. Refinement converged at $R = 0.0358$, $R_w = 0.0395$, where $w = [\sigma^2(F) + 0.00044F^2]^{-1}$, with no final shifts greater than 0.2σ. The largest residual electron density was 1.1 e Å^{-3} close to a Sn atom.

The final positional parameters are given in Table 2, selected bond parameters for the anion are in Table 3, and the anion geometry is illustrated in Figs. 2 and 3. For all three crystallographic studies complete lists of bond lengths and angles, thermal parameters and structure factors are available from the authors.
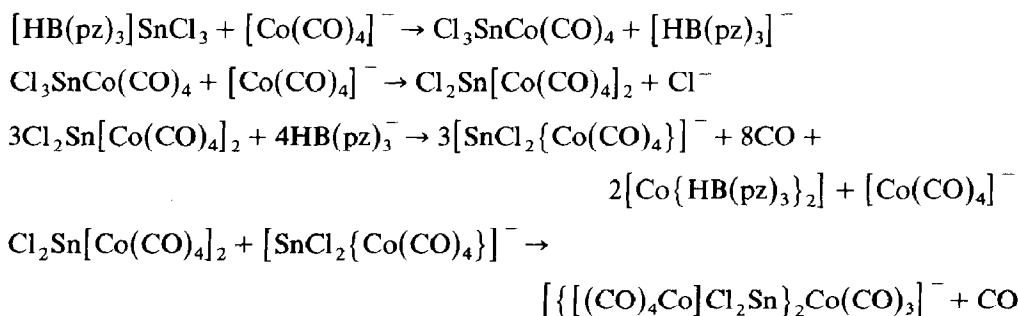
EHMO calculations

Extended Hückel Molecular Orbital calculations [16] were performed by use of the standard program ICON8 [17]. The calculations were carried out on a range of molecules *trans*-(X)(CO)$_3$CoSiCl$_3$, including X = CO, NH$_3$, PCl$_3$, SiCl$_3$. Silicon was used as the group 14 element rather than tin, since more reliable orbital parameters are available for the lighter elements; the qualitative conclusions are assumed to apply also to the tin species in view of the generality of the bond-shortening effects. Calculations were performed with and without the inclusion of silicon d-orbitals. The results are described more fully elsewhere [18].

Results and discussion

Although Me$_3$SnCl reacts with [HB(pz)$_3$]$^-$ to give Me$_3$Sn[(pz)$_3$BH] by chloride replacement [19], the corresponding reaction between ClSn[Co(CO)$_4$]$_3$ and [HB(pz)$_3$]$^-$ has been shown previously not to proceed analogously; instead [{[(CO)$_4$Co]$_2$ClSn}$_2$Co(CO)$_3$]$^-$ was produced, as the [Co{(pz)$_3$BH}$_2$]$^+$ salt [6], via a complicated series of disproportionation and coupling reactions. We have now examined the corresponding reaction of the bidentate ligand [H$_2$B(pz)$_2$]$^-$ with

ClSn[Co(CO)$_4$]$_3$. This gives initially a red solution in thf, which after evaporation and extraction yields an intense green solution. The infrared spectrum of this shows ν(CO) bands assignable to Sn[Co(CO)$_4$]$_4$ and the anion [{[(CO)$_4$Co]$_2$ClSn}$_2$ Co(CO)$_3$]$^-$, neither of which is green. Attempts to isolate either of these species from the complicated mixture were thwarted by decomposition. However, as with the tridentate ligand, it appears that [(pz)$_2$BH$_2$]$^-$ displaces a [Co(CO)$_4$]$^-$ from ClSn[Co(CO)$_4$]$_3$, which can then couple with another molecule of ClSn[Co(CO)$_4$]$_3$ to give Sn[Co(CO)$_4$]$_4$. Presumably [Sn{Co(CO)$_4$}$_2$Cl]$^-$ is also formed as an intermediate, and replaces a CO ligand of another molecule of ClSn[Co(CO)$_4$]$_3$ to give the anion [{[(CO)$_4$Co]$_2$ClSn}$_2$Co(CO)$_3$]$^-$. The reactions of [H$_2$B(pz)$_2$]$^-$ and [HB(pz)$_3$]$^-$ with ClSn[Co(CO)$_4$]$_3$ are therefore broadly similar in giving a mixture of several species, some of which are very unstable. However in neither of these systems is there any indication of the formation of a *closo*-SnCo$_3$ cluster.

An alternative approach to the synthesis of a sterically crowded SnCo$_3$ unit involves the possible coupling of [HB(pz)$_3$]SnCl$_3$ with [Co(CO)$_4$]$^-$. However when these were brought together in thf a number of colour changes occurred to give a red solution from which fractional crystallisation gave a 10% yield of [Co{(pz)$_3$ BH}$_2$][{[(CO)$_4$Co]Cl$_2$Sn}$_2$Co(CO)$_3$] which was identified by X-ray crystallography. This species is orange coloured, and has a different ν(CO) spectrum from that of the crude extract, so it is not a major initial product in the system. Again several reactions have taken place, including dissociation of [HB(pz)$_3$]$^-$ from the tin atom, conversion of a Sn–Cl into a Sn–Co(CO)$_4$ bond, formation of Co^{III} as [Co{(pz)$_3$BH}$_2$]$^+$, and replacement of a CO ligand on cobalt by a [SnCl$_2${Co(CO)$_4$}]$^-$ moiety. The probable route to the anion seems to be:

$$[HB(pz)_3]SnCl_3 + [Co(CO)_4]^- \rightarrow Cl_3SnCo(CO)_4 + [HB(pz)_3]^-$$

$$Cl_3SnCo(CO)_4 + [Co(CO)_4]^- \rightarrow Cl_2Sn[Co(CO)_4]_2 + Cl^-$$

$$3Cl_2Sn[Co(CO)_4]_2 + 4HB(pz)_3^- \rightarrow 3[SnCl_2\{Co(CO)_4\}]^- + 8CO +$$

$$2[Co\{HB(pz)_3\}_2] + [Co(CO)_4]^-$$

$$Cl_2Sn[Co(CO)_4]_2 + [SnCl_2\{Co(CO)_4\}]^- \rightarrow$$

$$[\{[(CO)_4Co]Cl_2Sn\}_2Co(CO)_3]^- + CO$$

To test part of this sequence a deficiency of [HB(pz)$_3$]$^-$ was added to a solution of Cl$_2$Sn[Co(CO)$_4$]$_2$ in thf. On work-up, the hexane-soluble ClSn[Co(CO)$_4$]$_3$ (formed by coupling of the displaced [Co(CO)$_4$]$^-$ with Cl$_2$Sn[Co(CO)$_4$]$_2$) was found, together with the expected anion (2).

The reaction of five-coordinate [H$_2$B(pz)$_2$]SnCl$_3$ with an excess of [Co(CO)$_4$]$^-$ also gave spectacular colour changes, with the major final product being a green, very air-sensitive anion. The only positively identified species was Co[(pz)$_2$BH$_2$]$_2$, which remained when the other components had been lost.

What appears to be the same green anion was produced in the reaction of Sn[Co(CO)$_4$]$_4$ with either [HB(pz)$_3$]$^-$ or [H$_2$B(pz)$_2$]$^-$. By analogy with the outcome of the reactions of ClSn[Co(CO)$_4$]$_3$ and Cl$_2$Sn[Co(CO)$_4$]$_2$ with these ligands, as described above, we expected this reaction to give the anion [{[(CO)$_4$Co]$_3$Sn}$_2$Co-(CO)$_3$]$^-$, and the ν(CO) frequencies are not inconsistent with a sequence [{[(CO)$_4$Co]Cl$_2$Sn}$_2$Co(CO)$_3$]$^-$ $\rightarrow$ [{[(CO)$_4$Co]$_2$ClSn}$_2$Co(CO)$_3$]$^-$ $\rightarrow$ [{[(CO)$_4$-

Co]$_3$Sn$_2$Co(CO)$_3$]$^-$. However the first two anions are not particularly air-sensitive, and there is no reason why replacing the final Cl on Sn by another Co(CO)$_4$ unit would give a less stable species; [{[(CO)$_4$Co]$_3$Sn}$_2$Co(CO)$_3$]$^-$ would be no more sterically crowded than Sn[Co(CO)$_4$]$_4$. An intense green colour is also not really expected for an anion of the type [{[(CO)$_4$Co]$_3$Sn}$_2$Co(CO)$_3$]$^-$ by comparison with earlier members in the series, so the identity of the product of these reactions remains unresolved.

The anions from these reactions that have been characterised apparently arise through displacement of the *trans*-CO of a Co(CO)$_4$ group by a Lewis base of the type [SnX$_3$]$^-$. To study such a reaction in a simpler system, and to provide an extended series of anions for structural comparisons, Cl$_3$SnCo(CO)$_4$ was treated with [SnCl$_3$]$^-$. A fairly rapid reaction took place at room temperature, and the expected anion [(Cl$_3$Sn)$_2$Co(CO)$_3$]$^-$ (1) was isolated as its Et$_4$N$^+$ salt. However the relatively low yield (20%), and the changes in ν(CO) frequencies, show that even this system is complicated by side reactions.

The structures of both new anions, [{[(CO)$_4$Co]Cl$_2$Sn}$_2$Co(CO)$_3$]$^-$ (2) and [(Cl$_3$Sn)$_2$Co(CO)$_3$]$^-$ (1) were determined by single crystal X-ray diffraction studies. [{[(CO)$_4$Co]Cl$_2$Sn}$_2$Co(CO)$_3$]$^-$ was isolated as the [Co{(pz)$_3$BH}$_2$]$^+$ salt and crystallised from CH$_2$Cl$_2$/benzene with the anion lying on a two-fold axis and the cation lying on an inversion centre. There is also a molecule of benzene in the lattice, also lying about an inversion centre. The structure of the [Co{(pz)$_3$BH}$_2$]$^+$ cation is the same as that found previously [6], with a near-regular octahedral environment at the Co atom. The geometry of the anion 2 is illustrated in Fig. 1. It consists of a planar central Co(CO)$_3$ unit with two SnCl$_2$[Co(CO)$_4$] units bonded in a *trans* arrangement. A view along the Sn–Co–Sn direction (Fig. 3) shows that the substituents are staggered with respect to the equatorial carbonyl groups. The bond lengths and angles are discussed in detail below.

The lattice adopted by Et$_4$N[(Cl$_3$Sn)$_2$Co(CO)$_3$] contains two independent anions, each lying on a two-fold axis; the asymmetric unit therefore contains two half-anions and one cation. The two independent anions do not differ significantly, so the discussion refers to average values of the parameters. The geometry of the anion 1 is illustrated in Fig. 2, which shows two SnCl$_3$ ligands bonded *trans* to each other about the planar Co(CO)$_3$ unit. The projection of this anion along the Sn–Co–Sn vector shows that the Sn–Cl bonds virtually eclipse the Co–CO$_{eq}$ bonds (Fig. 3).

The series of anions 1–3 allow interesting comparisons to be made, and average selected bond parameters are given in the structural diagrams. As noted above, the relative orientations of the substituents on Sn and on Co vary from near-eclipsed for 1, to near-staggered for 3, through intermediates between these extremes for 2, (Fig. 3). This suggests the Sn–Co distance is sufficiently long to ensure there is negligible interaction between the groups on the tin atoms and the equatorial carbonyl groups on the central cobalt atom. This is also supported by the essentially linear Sn–Co–Sn arrangement in all three anions, including the unsymmetrical 2 and 3.

The most notable feature for the anions is the very short Sn–Co distances for the *trans* tin atoms, varying from 2.444 Å in 1 (the shortest bond between a tin and a transition metal yet reported) to 2.508 Å in 3. These compare with distances of 2.562 and 2.662 Å, respectively, for the Sn–Co bonds to the outer Co(CO)$_4$ groups of 2 and 3, which are more normal; the Sn–Co bond lengths for ClSn[Co(CO)$_4$]$_3$

and $BrSn[Co(CO)_4]_3$ average 2.60 Å, while those in $Cl_2Sn[Co(CO)_4]_2$ are 2.534(1) Å [20]. In other words, replacement of a *trans*-CO ligand by a *trans*-$[SnX_3]^-$ group leads to a shortening of the opposite Sn–Co bond. A similar effect was observed for the anion $[\{(CO)_9Co_3Ge\}_2Co(CO)_3]^-$ which has short Ge–Co bonds *trans* to each other (2.288 Å) [21]. This effect is not related to the overall charge on the species involved, since an analogous effect is seen in the shortening of the Si–Mn bond on going from $Me_3SiMn(CO)_5$ to $Me_3SiMn(CO)_4(PPh_3)$ (2.497 to 2.453 Å [22]), and a similar effect on the Sn–Mn bond has been observed going from $Ph_3SnMn(CO)_5$ to $Ph_3SnMn(CO)_4(PPh_3)$ (2.674 to 2.627 Å [23]). For all these species a CO group has a larger *trans*-influence than a ligand with a group 14 or 15 donor atom.

One explanation often advanced for this type of bond shortening invokes d_π–d_π bonding in the metal–metal bond. When a good π-acceptor such as CO *trans* to the metal–metal bond is replaced by a weaker π-acceptor ligand such as $[SnX_3]^-$, the filled $3d_\pi$ electrons on cobalt would become available for overlap with the vacant d_π orbitals on the tin atom, thus strengthening and shortening the Sn–Co bond [22–24]. (A variation on this theme would involve $d_\pi \rightarrow \sigma^*$ bonding, cf. P–M bonding [25]). However despite many studies, both experimental and theoretical, there is no real evidence that d_π–d_π bonding is other than a minor effect in bonds between group 14 atoms and transition metals [24].

To analyse the bonding in more detail EHMO calculations were performed [16–18]. The model systems chosen for the calculations were $Cl_3SiCo(CO)_4$ and $[(Cl_3Si)_2Co(CO)_3]^-$ because input parameters are more reliably known for silicon than for tin, but the conclusions are expected to be applicable to the anions **1–3** since these shortening effects seem quite general. The first conclusion that can be drawn from the calculations is that any d_π–d_π or d_π–σ^* bonding in the Si–Co bond is minor for both species, and so is unlikely to be responsible for the changes in bond lengths; instead the important feature is the Si–Co σ bond, and in particular the hybridisation of the cobalt atom.

For a *trans*-$X_2Co(CO)_3$ species the Co–X bonds will be formed using hybrid orbitals combining the $3d_{z^2}$, the $4s$ and the $4p_z$ orbitals from cobalt, with the $4s$ contribution a minor one. The $3d_{z^2}$ orbital is lower in energy than the $4p_z$, and will have radial maxima closer to the cobalt atom than those of the $4p_z$ orbital. For a symmetrical species each Co–X bond will involve the same relative contributions from the $3d_{z^2}$ and the $4p_z$ orbital.

We now consider *trans*-$(R)(X)Co(CO)_3$, where R is a good σ-donor and X is a poor σ-donor. In this case the relative amounts of $3d_{z^2}/4p_z$ in each of the cobalt hybrid orbitals pointing towards R and X will be apportioned so as to provide the best overall interactions with both species. The smaller, lower energy, $3d_{z^2}$ orbital will concentrate in the hybrid pointing towards the poorer σ-donor X, since it will provide the best energy match, while the hybrid directed towards the better σ-donor R (i.e. the one with the higher energy lone pair) will incorporate more $4p_z$. Since the $4p_z$ orbital will provide maximum overlap further from the cobalt atom, the bond to R will be lengthened and that to X shortened, relative to those for the hypothetical case in which each hybrid contains the same relative amounts of $3d_{z^2}/4p_z$.

This then accounts for the short bonds in the anions **1–3**. CO has a low-energy σ-pair, so in $R_3SnCo(CO)_4$ the Co–CO bond has an enhanced $3d_{z^2}$ contribution, so is short, while the Co–Sn bond opposite contains more $4p_z$ character and is thus lengthened. For the anions $[(R_3Sn)_2Co(CO)_3]^-$, each Co–Sn bond will involve the

same amounts of $3d_{z^2}$ and $4p_z$ character, thus each will have relatively more $3d_{z^2}$ than the Co–Sn bond in $R_3SnCo(CO)_4$ and so will be shortened. The same arguments can be used to account for the shortening of the Si–Mn bond when the poor σ-donor *trans*-CO in $Me_3SiMn(CO)_5$ is replaced by the better σ-donor PPh_3 to give $Me_3SiMn(CO)_4(PPh_3)$, and to also explain the other examples given earlier.

This rationalisation is essentially an "isovalent rehybridisation" argument of the type that has been previously applied to explain the *trans*-influence in platinum(II) complexes [26], and also the bond variations in early transition metal complexes [27], although the detailed conclusions from one system cannot be transferred directly to those with different geometries and oxidation states in which the relative energies of the orbitals involved are changed.

Another feature within the series of anions **1–3** is the geometry about the tin atoms. For $[(Cl_3Sn)_2Co(CO)_3]^-$ the Co–Sn–Cl angles are 116–120°, while the Cl–Sn–Cl angles are 97–101°, all significantly different from the 109° expected for tetrahedral tin. There are no particular steric constraints, and again ideas based on rehybridisation (Bent's rule [28]) provide the best rationale. The electronegative Cl atoms will attract excess p character in the hybrid orbitals tin uses to bond to them, leading to a decrease in the Cl–Sn–Cl angles. This will enhance the s character in the remaining orbital used by tin to bond to the cobalt atom, which will also contribute to the shortening of the Sn–Co bond; this feature partly explains the decrease in Sn–Co on going from **3** to **1**, as more electronegative groups replace the electropositive $Co(CO)_4$ groups. The angles about tin in **2** and **3** conform to the same general pattern, but analysis becomes more difficult as the symmetry decreases and steric interactions between $Co(CO)_4$ groups on the same tin atom become important.

Acknowledgements

References

1 G. Schmid, Angew. Chem. Int. Ed. Eng., 17 (1978) 392.
2 B.R. Penfold and B.H. Robinson, Accounts Chem. Res., 6 (1973) 73; D. Seyferth, Adv. Organometal. Chem., 14 (1976) 97.
3 G. Schmid, V. Batzel and G. Etzrodt, J. Organomet. Chem., 112 (1976) 345; R. Boese and G. Schmid, J. Chem. Soc., Chem Commun., (1979) 345; G. Etzrodt and G. Schmid, J. Organomet. Chem., 169 (1979) 259.
4 K.H. Whitmire, J.S. Leigh and M. Gross, J. Chem. Soc., Chem. Commun., (1987) 926.
5 J.T. McNeese, S. Wreford, L.D. Tipton and R. Bau, J. Chem. Soc., Chem. Commun., (1977) 390; H.J. Haupt, A. Gotze and U. Florke, Z. Anorg. Allgem. Chem., 557 (1988) 82; H.J. Haupt and U. Florke, Acta Cryst., C, 44 (1988) 472.
6 O.J. Curnow and B.K. Nicholson, J. Organomet. Chem., 267 (1984) 257.
7 S. Trofimenko, J. Am. Chem. Soc., 89 (1967) 3170.
8 S.K. Lee and B.K. Nicholson, J. Organomet. Chem., 309 (1986) 257.
9 D.J. Patmore and W.A.G. Graham, Inorg. Chem., 7 (1968) 771.
10 D.J. Patmore and W.A.G. Graham, Inorg. Chem., 5 (1966) 1405.

11 D.J. Patmore and W.A.G. Graham, Inorg. Chem., 5 (1966) 2222.

12 S. Trofimenko, J. Am. Chem. Soc., 89 (1967) 3148; M.R. Churchill, K. Gold and C.E. Maw, Inorg. Chem., 9 (1970) 1597.

13 S. Trofimenko, J. Am. Chem. Soc., 89 (1967) 3170.

14 P. Main, L. Lessinger and M.M. Woolfson, MULTAN77, University of York, 1977.

15 G.M. Sheldrick, SHELX76-Program for Crystal Structure Determination, University of Cambridge (U.K.), 1976.

16 A.G. Turner, Methods in Molecular Orbital Theory, Prentice-Hall, Englewood Cliffs, NJ, 1974.

17 R. Hoffman et al., ICON8, Quantum Chemistry Exchange Program.

18 M.J. Severinsen, M.Sc. Thesis, University of Waikato, Hamilton, NZ, 1986.

19 B.K. Nicholson, J. Organomet. Chem., 265 (1984) 153.

20 K.M. Mackay, B.K. Nicholson and M. Service, Acta Crystallogr., in press.

21 D.N. Duffy, K.M. Mackay, B.K. Nicholson and R. Thomson, J. Chem. Soc., Dalton Trans., (1982) 1029.

22 M.C. Couldwell and J. Simpson, J. Chem. Soc., Dalton Trans., (1976) 714.

23 R.F. Bryan, J. Chem. Soc. A (1967) 172.

24 K.M. Mackay and B.K. Nicholson, in G. Wilkinson, F.G.A. Stone and E. Abel (Eds.), Comprehensive Organometallic Chemistry Ch. 43, Pergamon, Oxford, 1982; J.A. Zubieta and J.J. Zuckerman, Prog. Inorg. Chem., 24 (1978) 251, and refs. therein.

25 A.G. Orpen and N.G. Conelly, J. Chem. Soc., Chem. Commun., (1985) 1310.

26 S.S. Zumdahl and R.S. Drago, J. Am. Chem. Soc., 90 (1968) 6669; see also T.G. Appleton, H.C. Clark and L.E. Manzer, Coord. Chem. Rev., 10 (1973) 341, and J.K. Burdett, Molecular Shapes, Wiley, New York, 1980.

27 K.D. Dobbs and W.J. Hehre, J. Am. Chem. Soc., 108 (1986) 4663.

28 H. Bent, Chem. Rev., 61 (1961) 275.